DOI 10.5162/12dss2015/P5.3

Microfluidic Measurement of Cell Motility in Response to Applied Non-homogeneous DC Electric Fields

Marisa Rio[1], Sharanya Bola[2], Richard H. Funk[2] and Gerald Gerlach[1]
[1]Institute for Solid State Electronics, TU Dresden, Dresden, Germany
[2]Department of Anatomy, TU Dresden, Dresden, Germany
Contact: marisa.rio@tu-dresden.de

Abstract
Endogenous electric fields play an important role in many biological processes. In order to gain an insight into these biological phenomena, externally applied electric fields are used to study cellular responses. In the present study, we report on the steps towards microfluidic biochip assembling and its application to murine photoreceptor-derived 661W cells. In this work we describe the construction of a microfluidic biochip, which intends to mimic the non-homogeneous endogenic electric fields near wounds *in vitro*. The device is easy to fabricate and enables live-cell imaging under an inverted microscope. The experimental results have shown that the microfluidic biochip is biocompatible and suitable for cellular electrotaxis experiments in non-homogeneous DC electric fields.

Key words: electric field strength, cell motility, electrotaxis; microfluidic biochip; photoreceptor-derived 661W cells

Introduction

Directed cell migration is essential in a variety of biological processes such as wound healing, cancer metastasis, regeneration and immune responses [1]. There are diverse external cues like chemokines, cell-cell contacts, growth factors and the extracellular matrix environment that regulate cell migration [2]. Less well recognized is the influence of endogenous electric fields (EFs). Nevertheless, it has been shown that they play an important role in many cell biological phenomena, ranging from cell adhesion, migration, embryonic and tissue development to wound healing [3-8]. Studies suggest that a large majority of the motile cells are electrically sensitive [5,9,10]. Upon externally applied electric fields within physiological strength, cell-directional migration towards the anode or the cathode can be induced. The direction of migration varies among cell types [4]. The mechanisms that drive the cells under EFs are still not very well understood. Therefore, there is a need for a system which represents an *in vivo* electrical environment for elucidating the EF-directed cellular mechanisms. To date, the majority of electrotaxis devices had only minor changes since first introduced over 30 years ago [11,12]. Although using direct current (DC) supplies, experiments are generally performed in homogeneous EFs and, consequently, cells experience uniform EF strengths. However, *in vivo* cells experience non-homogeneous fields.
In this work, we describe the construction of a microfluidic biochip, which mimics the non-homogeneous EF environment near wounds *in vitro*.

Materials and Methods

Device fabrication

As depicted in Figure 1, the microfluidic biochip is composed of a polycarbonate (PC) base plate connected to a PDMS channel plate. The base plate houses the Ag/AgCl electrodes (World Precision Instruments, Berlin, Germany) each one connected to one end of a fluidic channel. Moreover, a SU-8 free-standing membrane seals the fluidic channels leaving only the central electrode opening, which connects each electrode to the central well. The setup is finalized by a PDMS cell chamber for cell stimulation.

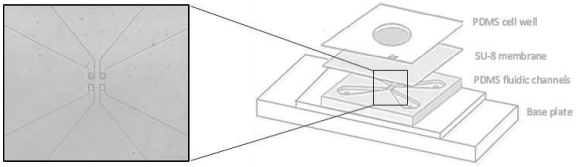

Fig. 1: Multilayer composition of the microfluidic biochip

with detail of the SU-8 membrane and its 25 µm electrode openings aligned over the fluidic channels ends

The microfluidic biochip fabrication encompasses three stages:

Step 1: Fabrication of the channel plate:
At first, a SU-8 master was fabricated using standard lithography. Briefly, in order to obtain 40 µm height channels, SU-8 3025 (MicroChem Corp., Newton, USA) was spin-coated at 500 rpm for 10 s and spread at 1000 rpm for 30 s. A baking step of 30 min at 95°C and an exposure to UV for 1 min followed. The post exposure bake was then performed at 65°C for 1 min and 95°C for 5 min. With the purpose of prolonging the masters' lifetime and facilitate PDMS removal from the mold, the master was exposed to (Tridecafluoro-1,1,2,2-Tetrahydrooctyl)-1-Trichlorosilane (United Chemical Technologies, USA) atmosphere for 2 h.
The silanized silicon master was then used to pattern the microfluidic channels by soft lithography. Polydimethylsiloxane (PDMS) (Sylgard 184 Silicone elastomer, Dow Corning, Midland, USA) silicone base and curing agent were mixed in a 10:1 ratio by weight and degassed. The mixture was subsequently injected in the MicCell platform (GesiM, Großerkmannsdorf, Germany) over the PC base plate. The curing process was done at 100°C for 60 min. Once cured and cooled down, the MicCell platform was disassembled releasing the base plate with the fluidic channel built in the PDMS polymer.

Step 2: Fabrication of the SU-8 free-standing membrane:
The membrane is responsible for sealing the microfluidic channels and enabling the enclosed electrolyte solution to flow through the openings up to the cell culture chamber. Once the device demands for an optically transparent and biocompatible [13] membrane, a lift-off technique using SU-8 and standard photolithography was selected. Additionally, this method facilitates obtaining high resolution geometric patterns. In order to facilitate the SU-8 patterned membrane release from the substrate a sacrificial layer OmniCoat™ (MicroChem Corp., Westborough, USA) was spin coated and soft baked prior to resist deposition. The following photolithographic steps were processed as previously described only with minor adjustments to obtain an 80 µm thick photoresist layer. During the development step, the solution was gently stirred not to introduce additional mechanical stresses, until the lift-off process was complete.

Step 3: Multilayer integration:
Lastly, the channel plate, the SU-8 free-standing membrane and the cell chamber were assembled. A covalent bonding of the PDMS fluidic channels to the SU-8 membrane is important for a leakage-free device. With that concern, a surface functionalization of the SU-8 free standing membrane was performed. This was a two steps process: first the SU-8 surface was activated by O_2 plasma (100 W, 150 sec 100 W). Subsequently, the plasma treated layer was soaked in 5% APTES (Sigma-Aldrich, Munich, Germany) solution and heated at 40°C on a hotplate for 20 min. The APTES solution is responsible for introducing a silanized layer on the substrate, forming amine groups on the SU-8 surface. Meanwhile, the PDMS channel plate was activated by O_2 plasma (same parameters). At this point, the functionalized SU-8 membrane was aligned over the fluidic channels using an optical microscope and subsequently placed over a hotplate for bonding. The optimized bonding temperature and time for our experiments were 70°C and 10 min, respectively. During the bonding process, the activated amine and silanol groups condense to reduce their surface free energy. Consequently, Si-O-Si covalent bonds are formed between the SU-8 and PDMS pieces, leading to strong, irreversible bonding of the two materials [14].
At last, the cell chamber was prepared by cutting a slab of PDMS (22 mm^2) and punching it in the middle with 8 mm diameter biopuncher Harris, Uni-Core™ (Ted Pella, Redding, USA). The PDMS provides a watertight reversible sealing mediated by van der Waal forces, enabling a functionalization free bonding.
The current in the DC microfluidic biochip makes its path from the Ag/AgCl electrodes via the electrolyte medium which fills the channels to the central well chamber.

Cell culture

Retinal cell culture of murine photoreceptor-derived 661W cells were cultivated under standard conditions (37°C, 5% CO_2) and allowed to grow for 24 h on polyethyleneterephthalate (PET) track-etched membranes (0.4 micron pores, BD Falcon™). After the incubation period, the membrane was placed in the microfluidic biochip for stimulation.

Cell viability

Cell viability was measured using the LIVE/DEAD assay kit (Invitrogen, California, USA). After EF-treatment, cells were washed with PBS containing 0.5 µM of calcein AM and 6 µM of ethidium homodimer-1 (EthD-1) and were incubated at 37°C with 5% CO_2 for 15 min. The staining solution was removed and the samples were then viewed under Olympus IX81 inverted microscope with 494 nm (green, Calcein) and 528 nm (red, EthD-1) excitation filters. Images were captured using Xcellence software (Olympus).

Immunofluorescence

Cells were washed with PBS (pH 7.2-7.4), fixed in 4% paraformaldehyde for 5 min at room temperature (RT), permeabilized with 0.5% Triton X-100 for 6 min and subsequently blocked with 2% bovine serum albumin (BSA) for 30 min. To detect focal contacts cells were incubated with mouse anti-human vinculin (1:200, Serotec, Martisried, Germany) at 4°C overnight. After the incubation time, cells were washed with PBS and later incubated with a fluorescein-isothiocyanate (FITC)-coupled goat anti-mouse antibody (1:1500, Dianova, Hamburg, Germany) along with tetramethylrhodamineisothiocyanate (TRITC)-conjugated phalloidin (1:300, Sigma Aldrich, Munich, Germany) at RT for 1 hour. TRITC was added to visualize actin. Finally, the nuclei were stained with 4‘6-diamidino-2-phenylindole dihydrochloride, DAPI (1:5000, Sigma-Aldrich, Munich, Germany) at RT for 5 min. Cells mounted in DABCO were imaged under fluorescence microscopy.

Time lapse

A real-time observation system consisting of an inverted Olympus microscope IX81 series; a CCD camera (Olympus DP70); the Xcellence imaging software together with an incubation system were used for observation of the cell migration at the microfluidic biochip. Images were recorded every 3 min for the duration of the experiment and a time-lapse video was created.

Cell tracking and evaluation of cell migration

For data analysis, captured images were imported into ImageJ (ImageJ 1.37v by W. Rusband, National Institutes of Health, Baltimore, USA). Image analysis was carried out by manual tracking and chemotaxis tool plug-in (v. 1.01, distributed by ibidi, Munich, Germany) in ImageJ software. We obtained the datasets of XY coordinates by manual tracking, and these datasets were imported into chemotaxis plug-in. This tool computed the cell migration speed and y-forward-migration index (y-FMI) of cells and plotted the cell migration pathway. The migration speed was calculated as an accumulated distance of the cell divided by time. The y-FMI of the cell was defined as the straight-line distance along the y-axis between the start position and the end position of cell divided by accumulated distance.

Results and discussion

Live-dead assay

The live-dead assay enables the differentiation of metabolic active cells from damaged and dead cells. Live and dead cells were checked for control as well as for stimulated samples using calcein and ethidium homodimer dyes. The biocompatible of the microfluidic device was confirmed as the cells exhibit no signs of apoptosis in both control and DC stimulation.

Electrotaxis experiment

The performance of the microfluidic biochip for electrotaxis studies was validated by studying the 661W cell line electrotactic response to non-homogenous DC EF stimulation (Figure 3).

The applied electric field was an average of 1 V/cm, resembling the fields observed in wound tissue [15]. This field induced a current in the order of 3 mA, which was stable during the duration of the experiment (120 min).

DOI 10.5162/12dss2015/P5.3

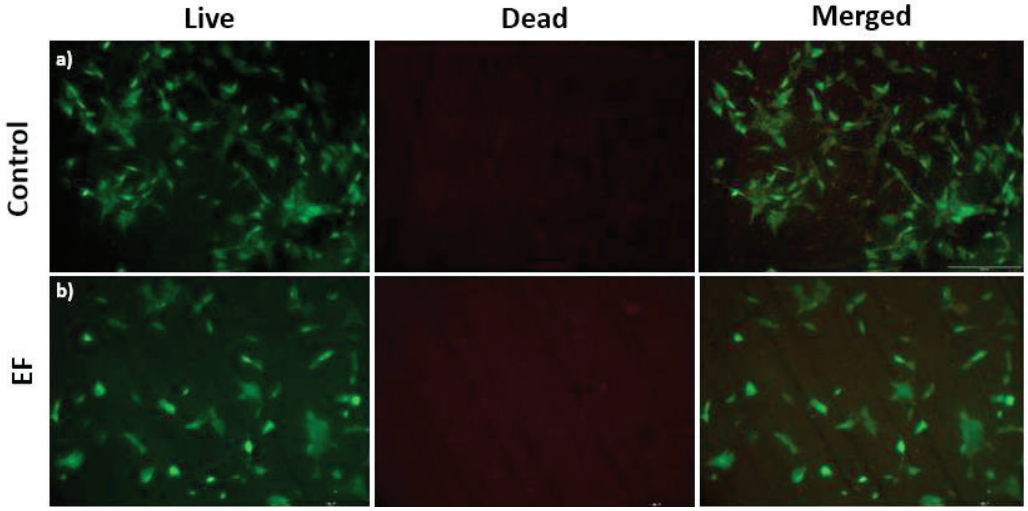

Fig. 2: Illustration of the cells after 120 min on device for a) control and b) EF. The green stain indicates viable cells, while red indicates non-viable. Scale bar 200 µm.

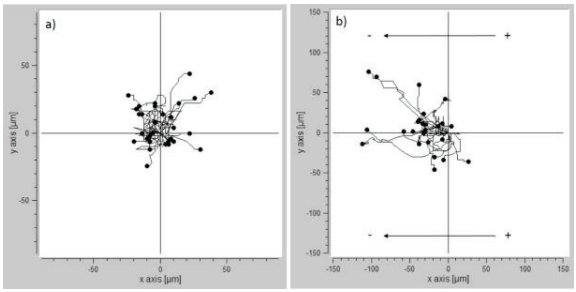

Fig. 3: Directional migration of 661w cell line for a) control and b) applied DC EF for cell tracks of a representative experiment

The migratory behavior of cells was recorded by taking images every 3 min for the duration of the experiment and subsequently creating a time-lapse video. The migration pathways were traced for both control and stimulated samples. In the absence of applied electric field (control samples, Fig. 3a) random migration in all directions with a scattered distribution was observed. Whereas, when a DC EF was applied, 661W cells preferentially migrated towards the cathode (Fig. 3b). Electrotactic migration was verified to be highly directional once almost all the cells migrated cathodally. The results confirm that the microfluidic biochip enables the application of physiologically relevant non-homogeneous electric fields to cells.

Immunofluorescence

Immunofluorescence labeling enables the visualization of cell biocompatibility parameters such as cell attachment and cell spreading, but also cytoskeleton organization and focal adhesion formation. The migration process encompasses a cascade of intracellular signaling events that coordinate actin polarization, protrusion, cellular and membrane polarization and adhesion mechanisms [16]. In Fig. 4 images from immunofluorescence labeling of control and stimulated samples are depicted. It is noticeable that the overall cellular orientation in Fig. 4b corresponds to the migration direction and the elongation perpendicular to the EF vector. In contrast to that, the orientation of the cytoskeleton (actin filaments) and the distribution of the focal contacts (vinculin) in Fig. 4a do not demonstrate to follow any directional cue.

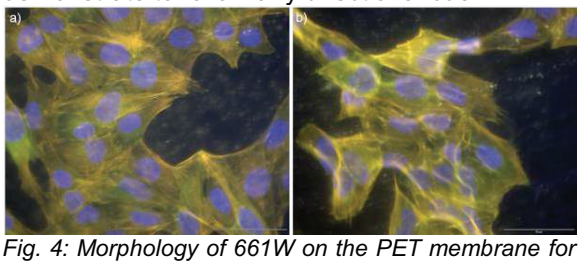

Fig. 4: Morphology of 661W on the PET membrane for a) control and b) applied EF. Cells were labeled for filamentous actin cytoskeleton (yellow due to the overlap of red stained actin and green stained vinculin), focal adhesion (green) and nucleus (blue). Scale bar 50 µm.

Numerical simulation of electric field and flow field

The electric field and flow field in the microfluidic biochip were numerically simulated using commercial software (ANSYS Maxwell 16). The DC conduction module was used in the electric field simulation. The resistivity of the medium at 37°C was set as 72 Ωcm for DMEM [17].

Conclusions

In this study a new electrotaxis microelectrode array was presented. In contrast with the current electrotaxis devices it has the advantage of permitting the use of non-homogenous direct current EFs that best mimic the *in vivo* environment near wounds.

The biocompatibility of photoreceptor-derived 661W cell line was tested on this device and its motility in the presence and absence of the applied electric field was verified. The movement of individual cells was tracked for the duration of the experiments, confirming the efficiency of cathodal-directed motility. Furthermore, immunofluorescence staining allowed the assessment of the adhesion efficiency.

In summary, this microelectrode array device has proven to be biocompatible and suitable for cellular electrotaxis experiments in non-homogeneous DC electric fields.

References

[1] J. Condeelis, J. Jones, and J.E. Segall, Chemotaxis of metastatic tumor cells: clues to mechanisms from the Dictyostelium paradigm, *Cancer Metastasis Rev.* 11, 55-68 (1992); doi: 10.1007/BF00047603

[2] F. Entschladen and K.S. Zänker, The migrationg cell, in Cell migration: signalling and mechanisms, *Karger*, 1-6. (2010); doi:10.1159/000274472

[3] M. Levin, Bioelectromagnetics in Morphogenesis, *Bioelectromagnetics* 24, 295-315 (2003); doi: 10.1002/bem.10104

[4] R. Nuccitelli, A role for endogenous electric fields in wound healing, *Current Topics in Developmental Biology* 58, 1-26 (2003); doi: 10.1016/S0070-2153(03)58001-2

[5] C.D. McCaig, A.M. Rajnicek, B. Song, and M. Zhao, Controlling cell behavior electrically: current views and future potential, *Physiological Reviews* 85, vol. 85, 943-978 (2005); doi: 10.1152/physrev.00020.2004

[6] M.A. Messerli and D.M Graham, Extracellular Electrical Fields Direct Wound Healing and Regeneration, *Biological Bulletin* 22, 79-92 (2011)

[7] K.R. Robinson and M.A. Messerli, Left-right, up/down: the role of endogenous electric fields as directional signals in development, repair and invasion, *Bioessays* 25, 759-766 (2003); doi: 10.1002/bies.10307

[8] R.H.W. Funk, T. Monsees, and N. Özkucur, Electromagnetic effects - From cell biology to medicine, *Progress in Histochemistry and Cytochemistry* 43, 177-264 (2009); doi: 10.1016/j.proghi.2008.07.001

[9] M. E. Mycielska and M. B. Djamgoz, Cellular mechanisms of direct-current electric field effects: galvanotaxis and metastatic disease, *Journal Cell Science* 117, 1631-1639 (2004); doi: 10.1242/jcs.01125

[10] F. Lin, F. Baldessari, C.C. Gyenge, T. Sato; R.D. Chambers, J.G. Santiago, E.C. Butcher, Lymphocyte Electrotaxis In Vitro and In Vivo, *The Journal of Immunology* 181, 2465-2471 (2008); doi: 10.4049/jimmunol.181.4.2465

[11] M.S. Keller, R.E. Cooper, Perpendicular orientation and directional migration of amphibian neural crest cells in dc electrical fields, *Proc. Natl Acad.*, 160-164 (1984); doi: 10.1073/pnas.81.1.160

[12] C.A. Erickson and R. Nuccitelli, Can be influenced by physiological electric fields embryonic fibroblast motility and orientation, *J. Cell Biol.* 98, 296-307 (1984); doi: 10.1083/jcb.98.1.296

[13] K.V. Nemani, K.L. Moodie, J.B. Brennick, A. Su, and B. Gimi, In vitro and in vivo evaluation of SU-8 biocompatibility, *Materials Science and Engineering C* 33, 4453–4459 (2013); doi: 10.1016/j.msec.2013.07.001

[14] P. Li, N. Lei, D.A. Sheadel, J. Xu, and W. Xue, Integration of nanosensors into a sealed microchannel in an hybrid lab-on-a-chip, *Sensors and Actuators B: Chemical*, 870-877 (2012); doi: 10.1016/j.snb.2012.02.047

[15] M, Zhao, B. Song, J. Pu,T. Wada, B. Reid, G.P. Tai, F. Wang, A.H. Guo, P. Walczysko, Y. Gu, T. Sasaki, A. Suzuki, J.V. Forrester, H.R. Bourne, P.N. Devreotes, C.D. MCaig, J.M. Penninger, Electrical signals control wound healing through phosphatidylinositol-3-OH kinase-gama and PTEN, *Nature* 442, 457–460 (2006); doi: 10.1038/nature04925

[16] C.Y. Funamoto, S. Firtel, R.A. Chung, Signaling pathways controlling cell polarity and chemotaxis, T*rends Biochem. Sci.* 26, 557-566 (2001); doi: 10.1016/S0968-0004(01)01934-X

[17] Y. Qu, R. Liao, and X. Zhang, "Real-Time Monitoring Primary Cardiomyocyte Adhesion Based on Electrochemical Impedance Spectroscopy and Electrical Cell-Substrate Impedance Sensing, *Anal. Chem.* 80, 990-996 (2008); doi: 10.1021/ac701745c

Acknowledgements

This work is part of the research program of the Research Training Group “Nano and Bio Techniques for the Packaging of Electronic Devices” financially supported by the German Research Foundation (DFG, GRK 1401).

The authors would like to thank Dr. Salvatore Girardo (Biotec, TU Dresden) for the help with the SU-8 free-standing membrane and for the fruitful discussions.